

SPITZER IRS SPECTRA OF YOUNG STARS NEAR THE HYDROGEN-BURNING MASS LIMIT

E. FURLAN,¹ N. CALVET,² P. D’ALESSIO,³ L. HARTMANN,² W. J. FORREST,⁴ D. M. WATSON,⁴ K. L. LUHMAN,² K. I. UCHIDA,¹
J. D. GREEN,⁴ B. SARGENT,⁴ J. NAJITA,⁵ G. C. SLOAN,¹ L. D. KELLER,⁶ AND T. L. HERTER¹

Received 2004 December 21; accepted 2005 January 31; published 2005 February 10

ABSTRACT

We present *Spitzer* Infrared Spectrograph measurements for two young stars near the hydrogen-burning mass limit in the Taurus star-forming region. While one of the objects, V410 X-ray 3, displays no mid-infrared excess, the other one, V410 Anon 13, shows a clear excess at wavelengths longward of 10 μm , indicative of a circumstellar disk. Moreover, the disk surrounding V410 Anon 13 is reminiscent of flared accretion disks around classical T Tauri stars; small dust grains in the disk photosphere generate the broad 10 μm silicate emission feature, whose structure suggests the presence of crystalline components. This demonstrates that very low mass objects, like their more massive counterparts, experience dust processing in their disks.

Subject headings: circumstellar matter — infrared: stars — stars: individual (V410 Anon 13, V410 X-ray 3) — stars: low-mass, brown dwarfs

Online material: color figure

1. INTRODUCTION

The first compelling evidence for the existence of protoplanetary disks was obtained when *IRAS* observations of T Tauri stars (~ 1 Myr, ~ 0.1 – $1 M_{\odot}$) revealed strong emission in excess of that expected from stellar photospheres (Rucinski 1985). The existence of these disks was later confirmed through direct imaging by the *Hubble Space Telescope* (O’Dell et al. 1993; Krist et al. 1998; Padgett et al. 1999). Disks have now been discovered around young stars covering a large range of masses, and even have been found among high-mass brown dwarfs (Comerón et al. 1998, 2000; Luhman 1999). Mid-IR studies of disks around low-mass stars and brown dwarfs performed from the ground have mostly used measurements in the L' band (3.8 μm ; see, e.g., Luhman & Rieke 1998; Liu et al. 2003; Jayawardhana et al. 2003). Observations with the *Infrared Space Observatory* added mid-IR photometry at 6.7 and 14.3 μm for many low-mass objects in ρ Oph and Chamaeleon (Comerón et al. 1998, 2000; Persi et al. 2000; Bontemps et al. 2001; Natta et al. 2002). Models used to reproduce disk emission around solar-mass pre-main-sequence stars have also been successfully applied to explain the spectral energy distributions (SEDs) of low-mass stars and brown dwarfs with excess emission (Natta & Testi 2001). However, only mid-IR spectra reveal details of the full mid-IR SED and test model parameters much better than broadband photometric studies, in which the SED is sampled coarsely and incompletely. The *Spitzer* Infrared Spectrograph (IRS) offers the opportunity to sample the entire mid-IR spectrum from 5 to 40 μm at un-

precedented levels of sensitivity; this wavelength range reveals disk emission at distances from a few tenths to a few AU from a low-mass star, which corresponds to a temperature range from about 500 K to somewhat below 100 K. IRS spectra not only constrain the properties of the inner regions of circumstellar disks in terms of physical structure but also in terms of composition, by measuring emission features associated with various dust species.

The Taurus star-forming region is an ideal region to observe circumstellar disks, since it is less dense than other star-forming regions like ρ Oph and thus suffers less from source confusion and extinction. The complex is nearby (~ 140 pc) and young (~ 1 – 2 Myr), making even very low mass objects bright enough for detection (see, e.g., Briceño et al. 1998). Two very low mass members of the Taurus cloud complex are V410 X-ray 3 and V410 Anon 13. They were first identified as late-type members of the Taurus star-forming region by Strom & Strom (1994), who performed a deep X-ray survey of the region around V410 Tau, supplemented by optical and near-IR photometry and spectroscopy. Both of these objects have optical spectral types near M6 (Briceño et al. 1998, 2002; Martín et al. 2001; Luhman et al. 1998) and masses near 0.1 M_{\odot} , according to theoretical evolutionary models (Briceño et al. 2002). In this Letter we show *Spitzer* IRS spectra of these two very low mass objects in Taurus. The spectrum of V410 Anon 13 is the first full mid-IR spectrum from 5 to 30 μm ever presented of an object near the hydrogen-burning mass limit with a circumstellar disk, whose structured silicate feature indicates the presence of crystalline components. In contrast, in V410 X-ray 3 the mid-IR emission is generated solely by the stellar photosphere.

2. OBSERVATIONS

We obtained spectra of two late-type members of the Taurus star-forming region, V410 X-ray 3 (M6) and V410 Anon 13 (M5.75), on 2004 February 7 with the IRS⁷ (Houck et al. 2004) on the *Spitzer Space Telescope* (Werner et al. 2004). We used both low-resolution IRS modules (Short-Low [SL] and Long-

¹ Center for Radiophysics and Space Research, 208 Space Sciences Building, Cornell University, Ithaca, NY 14853; furlan@astro.cornell.edu, kuchida@astro.cornell.edu, sloan@astro.cornell.edu, tlh10@cornell.edu.

² Harvard-Smithsonian Center for Astrophysics, 60 Garden Street, Cambridge, MA 02138; ncalvet@cfa.harvard.edu, hartmann@cfa.harvard.edu, kluhman@cfa.harvard.edu.

³ Centro de Radioastronomía y Astrofísica, UNAM, Apartado Postal 3-72 (Xan-gari), 58089 Morelia, Michoacán, México; p.dalessio@astrosmo.unam.mx.

⁴ Department of Physics and Astronomy, University of Rochester, Rochester, NY 14627; forrest@pas.rochester.edu, dmw@pas.rochester.edu, joel@pas.rochester.edu, bsargent@pas.rochester.edu.

⁵ National Optical Astronomy Observatory, 950 North Cherry Avenue, Tucson, AZ 85719; najita@noao.edu.

⁶ Department of Physics, Ithaca College, Ithaca, NY 14850; lkeller@ithaca.edu.

⁷ The IRS was a collaborative venture between Cornell University and Ball Aerospace Corporation, funded by NASA through the Jet Propulsion Laboratory and the Ames Research Center.

TABLE 1
 OBSERVING LOG

Name	R.A. (J2000.0)	Decl. (J2000.0)	Observing Mode	<i>Spitzer</i> AOR ID
V410 X-ray 3	04 18 07.96	+28 26 03.7	SL, LL, staring	3550976
V410 Anon 13	04 18 17.11	+28 28 41.9	SL, LL, staring	3551232

NOTE.—Units of right ascension are hours, minutes, and seconds, and units of declination are degrees, arcminutes, and arcseconds.

Low [LL], 5.3–14 and 14–40 μm , respectively, $\lambda/\Delta\lambda \sim 90$) in staring mode, which resulted in two exposures for each of the 2 orders of SL and of LL, separated by one-third of the slit length in the cross-dispersion (spatial) direction (see Table 1 for the observing log). In addition, we doubled the numbers of exposures taken; the total integration time amounted to 240 s in SL and 480 s in LL for each object.

The spectra were extracted and calibrated using the SMART software package (Higdon et al. 2004). First, the sky background was removed from each spectrum by subtracting observations taken in different orders of a certain module, but at the same nod position, from each other. Next, we used a variable-width column extraction in which the width of the column delineating the spectral profile varies linearly with wavelength, following the instrumental point-spread function. We extracted spectra of our calibrator star α Lac (A1 V) in the same way and obtained our final calibrated target spectrum by dividing the target by the calibrator spectrum and multiplying by the corresponding calibrator template spectrum (Cohen et al. 2003). Finally, we averaged the four spectra obtained for each module; the standard deviation of the mean was used to derive error bars for the spectra, as shown in Figure 1. To account for a small mispointing of part of our LL observation of V410 Anon 13, the second order of LL (14–20.9 μm) of its spectrum was scaled up by 10%, which resulted in a better match with the other modules. We estimate our absolute spectrophotometric accuracy to be of the order of 10%, while our relative accuracy is determined by the scatter of neighboring flux values; only spectral features above these fluctuations can be considered real. However, the wavelength region between 13.5 and 14.5 μm has to be treated with particular caution, since it is the area in which SL and LL meet; given the larger flux uncertainties at the order edges, in addition to possible small flux mismatches between SL and LL, only features

well above the noise level in this wavelength region can be identified with confidence.

3. ANALYSIS

Before examining the IRS spectra of V410 X-ray 3 and V410 Anon 13, we first review the previous evidence of circumstellar disks around these objects. One indication for accretion from a circumstellar disk is a broad H α emission line. The H α profile of V410 Anon 13 is broad and asymmetric, as expected from infalling accretion flows (Muzerolle et al. 2003); Muzerolle et al. (2000) derived an accretion rate of $\sim 5 \times 10^{-12} M_{\odot} \text{yr}^{-1}$ for this object. V410 X-ray 3 has a narrow and symmetric H α profile, as is found in weak-lined T Tauri stars, and thus is probably not accreting (White & Basri 2003). In addition to H α emission profiles, IR photometry can be used to assess the presence of circumstellar material. Strom & Strom (1994) found that V410 Anon 13 exhibited near-IR excess emission, as derived from their *J*, *H*, and *K* photometry of this object. Later measurements of the *K* – *L'* color of V410 Anon 13 (Luhman & Rieke 1998; Liu et al. 2003) confirmed this result; this object displays near-IR colors that exceed those expected from photospheric emission, as is the case for classical T Tauri stars, which are surrounded by optically thick accretion disks (see, e.g., Kenyon & Hartmann 1995). On the other hand, the near-IR colors of V410 X-ray 3 are consistent with a stellar photosphere alone.

In the comparison of our IRS spectra of V410 X-ray 3 and V410 Anon 13 in Figure 1, we find that the spectrum of V410 Anon 13 exhibits strong mid-IR excess emission, while the data for X-ray 3 are indicative of a photosphere with no disk, which is consistent with the previously published disk diagnostics for these objects. The most striking feature in our mid-IR spectrum of V410 Anon 13 is the broad emission feature centered around 10 μm , which is attributed to silicate grains suspended in the disk atmosphere, the superheated, optically thin surface layer of a flared disk. A flat, geometrically thin and optically thick disk would not produce any silicate emission feature.

In order to model the emission of V410 Anon 13, we need its stellar parameters. We adopt a spectral type of M5.75 and an effective temperature of 3000 K (Briceño et al. 2002; Luhman et al. 1998; Luhman & Rieke 1998). We estimated the extinction of V410 Anon 13 from the 0.8–2.5 μm spectrum obtained by Luhman et al. (2005). As shown in Figure 2, the spectrum of V410 Anon 13 is redder by $A_V = 5$ than that of V410 X-ray 3. Meanwhile, the near-IR spectrum of V410 X-ray 3 exhibits $A_V = 1$ relative to the M6 dwarf G1 406 (Luhman et al. 2005), while its optical spectrum and colors imply $A_V = 0.6$ (Luhman et al. 1998; Luhman 1999). We adopt $A_V = 0.8$ for V410 X-ray 3, and therefore $A_V = 5.8$ for V410 Anon 13. By combining this extinction with the *J*-band flux of this star and the bolometric correction for its spectral type, we arrive at a luminosity of $0.077 L_{\odot}$. With this luminosity

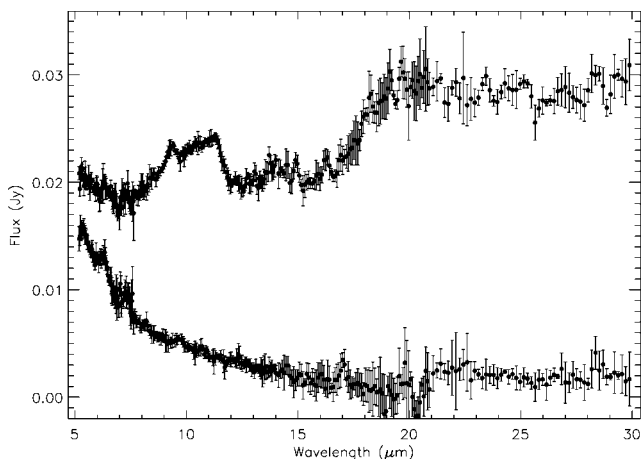


FIG. 1.—*Spitzer* IRS spectra of V410 Anon 13 (top) and V410 X-ray 3 (bottom). Both objects are plotted on the same scale. The error bars are derived from the standard deviation of the mean of four exposures per module.

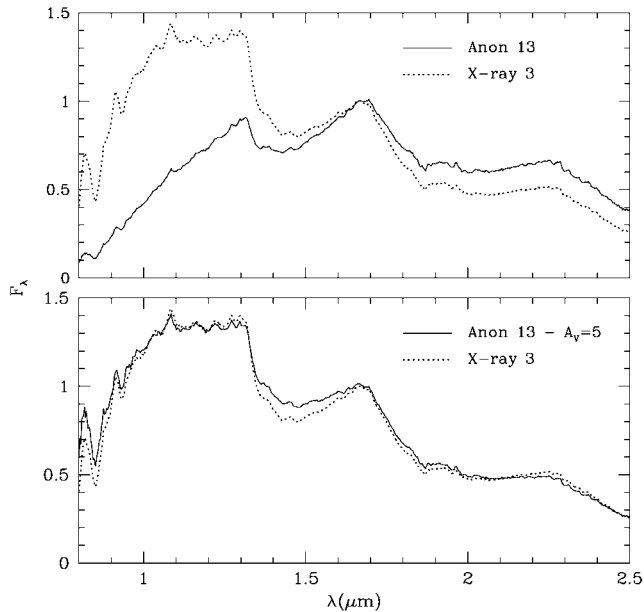


FIG. 2.—Near-IR spectra of V410 Anon 13 and V410 X-ray 3. The observed spectrum of V410 Anon 13 (*top*) has been dereddened to match the slope of V410 X-ray 3 (*bottom*), which implies that the extinction of the former is larger by an amount of $A_V = 5$. The spectra have a resolution of $R = 100$ and are normalized at $1.68 \mu\text{m}$.

and the adopted temperature, we derive a radius of $1.03 R_\odot$ for V410 Anon 13.

A model fit to the IRS spectrum of V410 Anon 13 is shown in Figure 3. It includes contributions from the star and a flared, dusty accretion disk irradiated by the central star. The stellar properties and the mass accretion rate are inferred from independent observations. The parameters for the star are a mass of $0.05 M_\odot$, a radius of $1.04 R_\odot$, and a luminosity of $0.077 L_\odot$ (in Fig. 3, the stellar photosphere is represented by one of the AMES-dusty models of Allard et al. 2001, which includes condensation, with $T_{\text{eff}} = 2900 \text{ K}$, $\log g = 3.5$). The accretion rate is very low, about $5 \times 10^{-12} M_\odot \text{ yr}^{-1}$ (Muzerolle et al. 2000). The remaining model parameters are determined by a comparison of the model to the observed spectrum. The disk model has been calculated following the procedures of D’Alessio et al. (2001), in which the vertical disk structure is derived self-consistently. The model also includes an inner disk “wall” illuminated frontally by the central object and located at the dust sublimation radius (at 4.7 stellar radii for a sublimation temperature of 1400 K for silicates). Interior to this wall, the disk is assumed to be free of dust. The height of the wall and the disk inclination angle affect the total flux emerging from the wall. Since the spectrum at wavelengths $< 6 \mu\text{m}$ is sensitive to the stellar and the wall spectrum, we can find for different disk inclinations a wall height that gives a wall spectrum that, when added to the stellar spectrum, fits the SED. Thus, we derive a wall height of 0.5 stellar radii. The presence of the 10 and $18 \mu\text{m}$ silicate bands in the IRS spectrum suggests that small silicate grains are responsible for the emission, and so we assume the grains to be interstellar-like dust grains composed of silicates and graphite. We further assume a minimum grain size of $0.005 \mu\text{m}$ and maximum size of $0.25 \mu\text{m}$, and a size distribution following the power law $n(a) \propto a^{-3.5}$. For the disk and wall emission, optical constants for silicates and graphite from Draine & Lee (1984) were used. The disk spectrum contribution becomes important for $\lambda > 6 \mu\text{m}$. The shape and strength of the $10 \mu\text{m}$ silicate band

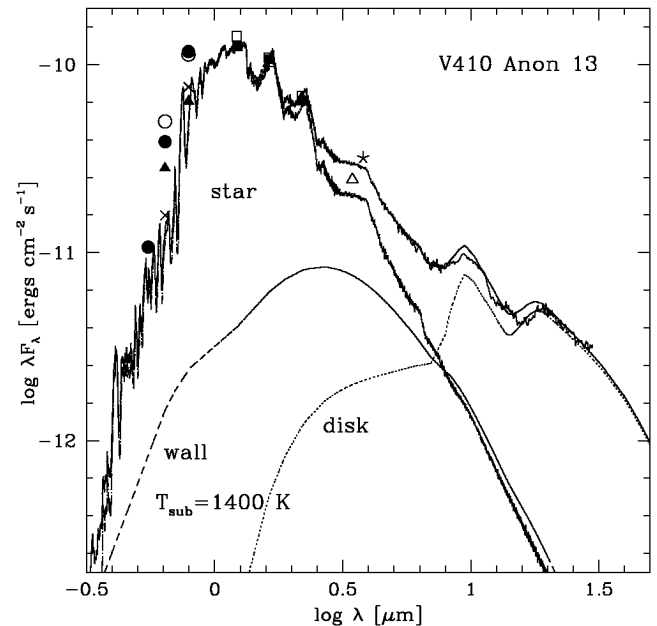


FIG. 3.—Model fitted to the IRS spectrum of V410 Anon 13 (gray; line segment from $\log \lambda = 0.7$ to 1.5). The stellar component is represented by one of the AMES-dusty models of Allard et al. (2001), which include condensation; T_{eff} is 2900 K , $\log g = 3.5$, and the stellar radius is $1.04 R_\odot$. The “wall” component represents the inner disk edge, located at the dust sublimation radius and illuminated frontally by the central object. Also shown are optical broadband observations from Strom & Strom (1994; *open circles*), Briceño et al. (1998; *filled circles*), Martín et al. (2001; *crosses*), Briceño et al. (2002; *filled triangles*), and near-IR observations from Strom & Strom (1994; *open rectangles*), Luhman & Rieke (1998; *open triangles*), Liu et al. (2003; *skeletal star*), and 2MASS (*filled rectangles*). These observations, in addition to the IRS spectrum of V410 Anon 13, have been corrected for reddening using Mathis’ reddening law (Mathis 1990) and $A_V = 5.8$. [See the electronic edition of the *Journal* for a color version of this figure.]

is sensitive to the dust composition and maximum grain size, while the continuum depends on the inclination angle. For our adopted dust composition and size distribution, an inclination angle of 70° fits the maximum flux of the $10 \mu\text{m}$ band best. A change in $\cos i$ from 0.3 to 0.5 would produce a $\sim 20\%$ increase in the maximum flux of the $10 \mu\text{m}$ band. For a given inclination angle, the depletion factor ϵ (i.e., the ratio between the dust-to-gas mass ratio in the disk atmosphere and the standard dust-to-gas mass ratio) affects the SED for $\lambda > 12 \mu\text{m}$ (P. D’Alessio et al. 2005, in preparation). To better fit the peak and the long-wavelength side of the $18 \mu\text{m}$ band, some dust settling is assumed in the model; an ϵ of 0.3 is adopted. An increase in ϵ from 0.3 to 1 increases the maximum flux at the $18 \mu\text{m}$ band by 70% , leaving the $10 \mu\text{m}$ band unaffected. The outer radius of the disk is set at 100 AU ; this value is arbitrary, since it is not constrained by the IRS part of the SED, and longer wavelength data are not available.

The continuum shape of the spectrum, which was corrected for extinction using the reddening law from Mathis (1990) with $A_V = 5.8$, is reproduced quite well with this model fit. There is excess emission above the continuum of the optically thick disk interior from about 8 to $30 \mu\text{m}$, because of silicate dust grains in the disk surface layer. The idea that objects near the hydrogen-burning limit could have flared disks like young, solar-mass stars is not new; in fact, both Natta et al. (2002) and Mohanty et al. (2004) concluded that some of the low-mass objects they observed in the ρ Oph star-forming region had mid-IR spectral energy distributions consistent with flared

disks. However, it is not clear whether young, low-mass objects with flared disks are representative of this class of objects; Apai et al. (2002) reported the detection of a mid-IR excess around Cha H α 2 (M5.25, 0.15 M_{\odot} ; Luhman 2004) that is consistent with a flat disk structure.

The structured emission peak around 10 μm indicates that crystalline silicates must be present in this disk; such structure has previously been observed in Herbig Ae/Be stars (e.g., Bouwman et al. 2001) and in classical T Tauri stars (e.g., Meeus et al. 2003; Forrest et al. 2004) and has been interpreted by changes in dust composition and also grain size. Depending on the environment, amorphous silicates are expected to generate a smooth feature with a FWHM of about 3 μm and a peak position between 9.6 and 9.9 μm (Bowey & Adamson 2002); additional dust components must be present in the disk of V410 Anon 13 to create the wide emission feature from 8 to 12 μm with its distinct peaks. To analyze the crystalline silicates in the dust around this object, we derived its opacity as a function of wavelength from the continuum-subtracted, extinction-corrected spectrum. It is interesting to note that the 8–14 μm opacity of V410 Anon 13 is nearly identical to that derived for FN Tau, a more massive classical T Tauri star in Taurus (B. Sargent et al. 2005, in preparation). Both objects display a well-pronounced peak at 9.35 μm , which is most likely generated by crystalline pyroxenes; the peak at 11.3 μm most likely indicates the presence of crystalline olivines, probably forsterite (Jäger et al. 1998). The structure between the 9.35 and 11.3 μm peaks could be caused by a combination of forsterite and pyroxene grains, since they both have structure in this wavelength region. The fact that the disk around V410 Anon 13 holds crystalline silicates shows that processing of

amorphous grains leading to the formation of crystalline silicates, like thermal annealing in inner regions of pre-main-sequence disks, also occurs in disks around very low mass objects.

4. CONCLUSIONS

We have presented mid-IR spectra from 5 to 30 μm of two young members of the Taurus star-forming region near the hydrogen-burning limit. One source, V410 X-ray 3, does not show any IR excess or veiling, and thus its spectrum can be regarded as emission by the photosphere. Meanwhile, V410 Anon 13 clearly displays a mid-IR excess as a result of emission by circumstellar material. These data comprise the first *Spitzer* IRS mid-IR spectrum of a disk around an object at the bottom of the stellar mass function. The slope of this spectrum is consistent with a flared structure, and the silicate emission band around 10 μm has a shape that indicates the presence of crystalline silicate components. Both of these characteristics are reminiscent of disks around solar-mass T Tauri stars.

This work is based on observations made with the *Spitzer Space Telescope*, which is operated by the Jet Propulsion Laboratory, Caltech, under NASA contract 1407. Support for this work was provided by NASA through contract number 1257184 issued by JPL/Caltech. K. L. was supported by grant NAG5-11627 from the NASA Long-Term Space Astrophysics program. This publication makes use of data products from the Two Micron All Sky Survey (2MASS), which is a joint project of the University of Massachusetts and IPAC/Caltech, funded by NASA and NSF.

REFERENCES

- Allard, F., Hauschildt, P. H., Alexander, D. R., Tamanai, A., & Schweitzer, A. 2001, *ApJ*, 556, 357
- Apai, D., Pascucci, I., Henning, Th., Sterzik, M. F., Klein, R., Semenov, D., Günther, E., & Stecklum, B. 2002, *ApJ*, 573, L115
- Bontemps, S., et al. 2001, *A&A*, 372, 173
- Bouwman, J., Meeus, G., de Koter, A., Hony, S., Dominik, C., & Waters, L. B. F. M. 2001, *A&A*, 375, 950
- Bowey, J. E., & Adamson, A. J. 2002, *MNRAS*, 334, 94
- Briceño, C., Hartmann, L., Stauffer, J., & Martín, E. 1998, *AJ*, 115, 2074
- Briceño, C., Luhman, K. L., Hartmann, L., Stauffer, J. R., & Kirkpatrick, J. D. 2002, *ApJ*, 580, 317
- Cohen, M., Megeath, S. T., Hammersley, P. L., Martín-Luis, F., & Stauffer, J. 2003, *AJ*, 125, 2645
- Comerón, F., Neuhäuser, R., & Kaas, A. A. 2000, *A&A*, 359, 269
- Comerón, F., Rieke, G. H., Claes, P., Torra, J., & Laureijs, R. J. 1998, *A&A*, 335, 522
- D'Alessio, P., Calvet, N., & Hartmann, L. 2001, *ApJ*, 553, 321
- Draine, B. T., & Lee, H. M. 1984, *ApJ*, 285, 89
- Forrest, W. J., et al. 2004, *ApJS*, 154, 443
- Higdon, S. J. U., et al. 2004, *PASP*, 116, 975
- Houck, J. R., et al. 2004, *ApJS*, 154, 18
- Jäger, C., Molster, F. J., Dorschner, J., Henning, Th., Mutschke, H., & Waters, L. B. F. M. 1998, *A&A*, 339, 904
- Jayawardhana, R., Ardila, D. R., Stelzer, B., & Haisch, K. E. 2003, *AJ*, 126, 1515
- Kenyon, S. J., & Hartmann, L. 1995, *ApJS*, 101, 117
- Krist, J. E., et al. 1998, *ApJ*, 501, 841
- Liu, M. C., Najita, J., & Tokunaga, A. T. 2003, *ApJ*, 585, 372
- Luhman, K. L. 1999, *ApJ*, 525, 466
- . 2004, *ApJ*, 617, 1216
- Luhman, K. L., Briceño, C., Rieke, G. H., & Hartmann, L. 1998, *ApJ*, 493, 909
- Luhman, K. L., McLeod, K. K., & Goldenson, N. 2005, *ApJ*, in press
- Luhman, K. L., & Rieke, G. H. 1998, *ApJ*, 497, 354
- Martín, E. L., Dougados, C., Magnier, E., Ménard, F., Magazzù, A., Cuillandre, J.-C., & Delfosse, X. 2001, *ApJ*, 561, L195
- Mathis, J. S. 1990, *ARA&A*, 28, 37
- Meeus, G., Sterzik, M., Bouwman, J. T., & Natta, A. 2003, *A&A*, 409, L25
- Mohanty, S., Jayawardhana, R., Natta, A., Fujiyoshi, T., Tamura, M., & Barrado y Navascués, D. 2004, *ApJ*, 609, L33
- Muzerolle, J., Briceño, C., Calvet, N., Hartmann, L., Hillenbrand, L., & Gullbring, E. 2000, *ApJ*, 545, L141
- Muzerolle, J., Hillenbrand, L., Calvet, N., Briceño, C., & Hartmann, L. 2003, *ApJ*, 592, 266
- Natta, A., & Testi, L. 2001, *A&A*, 376, L22
- Natta, A., Testi, L., Comerón, F., Oliva, E., D'Antona, F., Baffa, C., Comoretto, G., & Gennari, S. 2002, *A&A*, 393, 597
- O'Dell, C. R., Wen, Z., & Hu, X. 1993, *ApJ*, 410, 696
- Padgett, D. L., Brandner, W., Stapelfeldt, K. R., Strom, S. E., Terebey, S., & Koerner, D. 1999, *AJ*, 117, 1490
- Persi, P., et al. 2000, *A&A*, 357, 219
- Rucinski, S. M. 1985, *AJ*, 90, 2321
- Strom, K. M., & Strom, S. E. 1994, *ApJ*, 424, 237
- Werner, M. W., et al. 2004, *ApJS*, 154, 1
- White, R. J., & Basri, G. 2003, *ApJ*, 582, 1109